International Journal of Science and Research (IJSR)
ISSN (Online): 2319-7064
Index Copernicus Value (2013): 6.14 | Impact Factor (2014): 5.611

Synthesis and Characterization of Nanostructured $Mg(OH)_2$ and MgO

S. RSoniya[1], V. Manikantan Nair[2]

[1]Research Scholar, Department of Physics, Fatima Mata National College, Kollam-691001

[2]Department of Physics, Govt. College for Women, University of Kerala, Thiruvananthapuram

Abstract: ***Nanocrystalline oxides are of immense interest to scientists due to their enriched surface chemistry and high surface area. Among the metal oxide nanomaterials, magnesium oxide(MgO) is an exceptionally important material and has been extensively used in catalysis, toxic waste remediation, antibacterial materials, paints and superconductor products owing to its unique optical, electronic, magnetic, thermal, mechanical and chemical properties[1].In the present work magnesium hydroxide ($Mg(OH)_2$) nanostructures have been synthesized by the reaction of magnesium nitrate($Mg(NO_3)_2$) with sodium hydroxide (NaOH) in the presence of ethylene diamine tetra acetic acid (EDTA) via chemical precipitation method. The magnesium hydroxide sample was annealed at different temperatures to obtain samples of MgO of different grain sizes. The synthesis was carried out with the reaction mixture kept under uniform stirring using a magnetic stirrer. The magnesium hydroxide and magnesium oxide nanostructures were characterized by the method of XRD and FT Raman spectroscopy. The XRD peaks of $Mg(OH)_2$ obtained are very broad which gives a clear indication of small particle size. MgO samples were obtained by the heat treatment of the$Mg(OH)_2$ samples and as annealing temperature increases, the average grain size of nanocrystalline materials also increases[12]. The width of the X- ray diffraction pattern indicates the same results. FT Raman spectra of the samples were recorded and interpreted in comparison with the reported spectra of bulk crystals of $Mg(OH)_2$andMgO.***

Keywords: MgO, $Mg(OH)_2$, XRD, Raman spectrum

1. Introduction

The origin of the term nano comes from the Greek word "nanos" meaning dwarf and in scientific terms denotes one billionth of a unit. But the world of nanotechnology is definitely not a nano sized world. Nanotechnology world is swiftly evolving and opens up a new vista with enormous potential. The term nanotechnology was first used by late Professor Norio Taniguchi of University of Tokyo in 1974, and is defined as the design and fabrication of materials, devices and systems with control at nanometer dimensions. Nanotechnology is the manipulation of matter on an atomic and molecular scale. A more generalized description of nanotechnology was subsequently established by the National Nanotechnology Initiative, which defines nanotechnology as the manipulation of matter with at least one dimension sized from 1 to 100 nanometers. Nanotechnology as defined by size is naturally very broad, including fields of science as diverse as surface science, organic chemistry, molecular biology, semiconductor physics, micro fabrication etc. The associated research and applications are equally diverse, ranging from extensions of conventional device physics to completely new approaches based upon molecular self-assembly, from developing new materials with dimensions on the nanoscale to direct control of matter on the atomic scale.

Nano-science and nanotechnology (NT) are emerging fields of science and technology that they are witnessing surfacing of an increasing number of innovate ideas and applications. Nanoparticles as an integral part of nano-science represent the most visible applications of nanotechnology with commercial success. But there may hardly be very few areas of human life that will be exempted from the benefits of nanotechnology. The applications of nanotechnology range from health care (drug delivery, repair or reproduction of damaged tissues), water-treatment technologies (nanofiltration for water treatment), energy sector (increasing the efficiency of energy production, reduction of energy consumption), information and communications (memory storage, novel semiconductor devices, and quantum computers), industrial applications (aerospace, construction, nanoparticles in steel, glass, coatings, fire protection and detection), food industry (production, processing , safety, and packaging of food items), household (self cleaning glass and ceramic surfaces), textiles (water- and stain- repellent clothes), sports (materials for new athletic shoes, baseball bats tennis rackets, golf balls, sport towels, exercise mats), and agriculture sector, etc. Thus one of the key objectives of nanotechnology is to develop our knowledge to manipulate matter at nanoscale level to create novel, smart, cost effective and eco-friendly macrostructures to improve quality of human life.

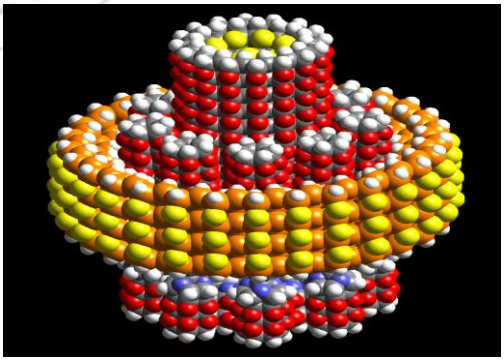

Figure 1: A typical nanostructure.

Making products at the nanometer scale is and will become a big economy for many countries. Meanwhile, according to the National Nanotechnology Initiative (NNI), scientists will create new ways of making structural materials that will be used to build products and devices atom-by-atom and molecule-by-molecule. These nanotechnology materials are

expected to bring about lighter, stronger, smarter, cheaper, cleaner, and more durable products[13].

In brief, Nanotechnology series explores all important developments of the past few years and thus aims to serve as an indispensable reference and educational tool for students, professionals, and everyone working in any field of the nano world by providing reliable up-to-date information in all areas of nano world.

In the project an attempt is made on the synthesis and characterization of nanostructured samples. The sample selected is the nanoparticles of the magnesium hydroxide [$Mg(OH)_2$] and magnesium oxide [MgO]. The nanoparticles of $Mg(OH)_2$ is synthesized through controlled chemical reaction of $Mg(NO_3)_2$ and NaOH in the presence of EDTA (Ethylene Diamine Tetra Acetic Acid). Nanocrystalline $Mg(OH)_2$ samples was used as precursor for the preparation of MgO. MgO samples were obtained by heating treatment of the $Mg(OH)_2$ samples[7]. The magnesium hydroxide sample was annealed at different temperatures to obtain samples of MgO of different grain sizes. The grain sizes of the samples are determined using Scherer's formula.

For different samples different XRD patterns will be obtained. The information obtained is compared with the JCPDS data of $Mg(OH)_2$ and MgO samples. The FT Raman spectrum of nanoparticles was also recorded and is compared with that of bulk crystal. This will give properties and structure of $Mg(OH)_2$ and MgO.

2. Experimental Methods

In the present study, nanoparticles of Mg $(OH)_2$ were synthesized through controlled chemical reaction between solutions containing Mg^{2+} and $(OH)^-$ ions in the presence of EDTA as stabilizer in the proper stochiometric ratio. The synthesis was carried out with the reaction mixture kept under uniform stirring using a magnetic stirrer. The white gel-like precipitate of nanoparticles of $Mg(OH)_2$ was centrifuged, and washed with distilled water and methanol several times to remove impurities present. The precipitate was then dried at 80 C and ground thoroughly using an agate mortar.

Nanocrystalline Mg $(OH)_2$ samples was used as precursor for the preparation of MgO. The magnesium hydroxide sample was annealed at different temperatures to obtain samples of MgO of different grain sizes. The sample codes, annealing temperatures and annealing time are given in the table 1.

Figure 2: Experimental Set-up

Table 1: Sample codes, annealing temperatures and annealing time

X_1	450	1
X_2	500	1
M_1	550	1
M_2	600	2

X-ray diffraction pattern provides a wealth of important information about the arrangement and spacing of atoms in a crystalline material. X-ray diffraction peaks are obtained satisfying the Bragg condition, $2d\sin\theta = n\lambda$, where, d is the interplanar distance, θ is the Bragg angle; n is a positive integer and λ is the wave length used. The intensity and position of the peaks give a clear idea of the structure of crystals. The average grain size of a sample can be calculated from the broadening of X-ray diffraction lines.

The average particle size, $= \frac{\lambda}{\beta \quad \theta}$, Where is the crystalline size in a direction perpendicular to the plane (hkl) corresponding to the measured reflection, λ is the wave length of X-ray used, K = 1 for spherical particles, β is the full width at half maximum in radian and θ is the Bragg angle. This formula is called Scherer's formula.

In the present study, X ray diffraction spectra of the sample of particles of $Mg(OH)_2$ and the two samples of MgO obtained by heat treatment of $Mg(OH)_2$ sample at 550 and 600 C (Samples M_1 and M_2) were recorded over the 2θ range from 20 to 70 .

The FT Raman spectra of nanoparticles of $Mg(OH)_2$ and the samples M_1 and M_2 were recorded using Bruker-FT Raman Spectrometer.

3. Result and Discussion

3.1 $Mg(OH)_2$

(i) X-ray diffraction pattern

The X-ray diffraction pattern of nanoparticles of Mg $(OH)_2$ is shown in Fig 3. The diffraction peaks indicate that the sample is crystalline in nature. The d values and intensity of peaks in the XRD pattern (Fig. 3) agree with JCPDS data of Mg $(OH)_2$ crystals. The comparison gave the result that the sample is exactly Mg $(OH)_2$ sample. The JCPDS data of Mg $(OH)_2$ crystal, and the d values and intensity of the sample obtained in the present study are given in the table 2.

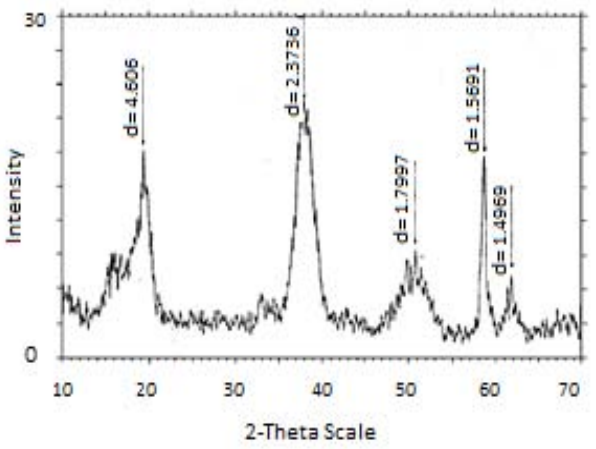

Figure 3: XRD pattern of nanostructured $Mg(OH)_2$sample

Table 2: JCPDS data values for $Mg(OH)_2$ crystals

d (A)	I	h	k	l
4.77	90	0	0	1
2.725	6	1	0	0
2.365	100	1	0	1
1.794	55	1	0	2
1.573	35	1	1	0
1.494	18	1	1	1
1.373	16	1	0	3
1.363	2	2	0	0
1.31	1	2	0	1
1.192	2	0	0	4
1.183	10	2	0	2
1.118	2	1	1	3
1.092	4	1	0	4
1.034	6	2	0	3
1.03	2	2	1	0
1.0067	8	2	1	1
0.9543	2	0	0	5
0.9503	6	1	1	4
0.9455	8	2	1	2
0.9085	4	3	0	0
0.9001	1	1	0	5
0.8974	2	2	0	4
0.8923	2	3	0	1
0.8643	6	2	1	3
0.8156	4	1	1	5
0.7865	4	2	2	0

The XRD peaks obtained were very broad. This is a clear indication of small particle size. As the peak broadens, the average particle size becomes smaller. The average particle size of the sample is calculated using Scherrer's formula and it is obtained as about 4 nm.

(ii) Raman Spectrum

The FT Raman spectrum of the sample of nanoparticles of $Mg(OH)_2$ is shown in Fig. 4. The peaks are obtained at frequencies 2932, 1415, 1094, 712, 451, 284 and 152 cm^{-1}. The peaks observed in the Raman spectrum of bulk $Mg(OH)_2$ reported in the literature and the peaks in the spectrum of nanocrystalline $Mg(OH)_2$ recorded in the present study are listed in table 3.

Table 3: The peaks observed in the Raman Spectrum

Bulk $Mg(OH)_2$ cm^{-1}	Nanocrystalline $Mg(OH)_2$ cm^{-1}
3652	2932
3688	1094
2696	712
725	451
443	284
277	152

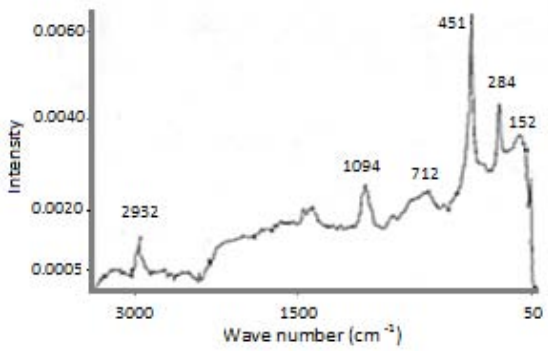

Figure 4: FT Raman spectrum of nanostructured $Mg(OH)_2$ sample

Magnesium hydroxide crystallizes into a layered type hexagonal lattice with one formula unit per primitive unit cell. The hydroxyl ions are oriented with their axis parallel to crystal C axis. Coblentz observed complex absorption bands in the 2500 – 4000 cm^{-1} region. These complex absorption bands lie in the region of hydroxyl ion stretching frequency. The crystal structure with its single formula unit per primitive unit cell leads to the prediction of only one infrared active hydroxyl stretching mode.

Factor group analysis of D_{3d}^3 space group predicts 4 Raman active and 4 IR active fundamentals. The structure of the irreducible representation of the internal rotational lattice and translational lattice (T) modes with their optical activities are

$$\Gamma_{int} = 1_{1}(\quad) + {}_{2}(\quad, \|)$$

$$\Gamma = 1(\quad) + (\quad, \perp)$$

$$\Gamma = 1_{1}(\quad) + 1(\quad) + {}_{2}(\quad, \|) + 1(\quad, \perp)$$

Where $\|$ and $\perp$ indicates parallel and perpendicular components.

The form of Raman tensors and the polarized Raman spectra of bulk crystals of $Mg(OH)_2$ are reported in literature.

The crystal structure of $Mg(OH)_2$ possesses a centre of inversion and the rule of mutual exclusion leads the presence of g-modes which are Raman active only. Since metal ions are located at centres of inversion, they do not take part in any of the Raman active g-modes whose normal co-ordinates are symmetric with respect to the inversion symmetry operation. Raman spectrum of single crystals of $Mg(OH)_2$ has been studied by N.B. Manson et al. The observed peaks are located at 3688, 3652, 2696, 725, 443,

and 227 cm^{-1}. The presence in the unit cell of two hydroxyl ions results in the Davydov-splitting of single hydroxyl stretching frequency into two components, a Raman active A_{1g} and an infrared active A_{2u} mode. Two hydroxyl stretching frequencies are observed at 3652 and 3688 cm^{-1}. These splitting of A_{1g} and A_{2u} modes are termed as factor group of Davydov-splittings. This is believed to be due in large measure to dipole interactions between vibrating ions.

Raman scattering spectrum of nanocrystalline$Mg(OH)_2$ is compared with that of bulk crystal. The peaks at 2696, 725, 443, and 227 cm^{-1} of bulk crystal are frequency shifted to 2932, 712, 451, and 284 cm^{-1} respectively in the case of nanocrystalline$Mg(OH)_2$ samples.

Reduction in the size of the crystals to very small values lead to the breakdown of law of conservation of momentum, which holds only strictly for large crystals. Vibrations modes corresponding to $k \neq 0$, where k is the wave vector, become allowed for very small crystals. This may lead to an increase in the width of the spectral lines of Raman scattering n the fundamental region, and to a frequency shift of the maxima of lines as compared with massive crystals.

The uniqueness of nanoparticles lies in their large surface-to-volume ratio. This is the reason that as size of the particle decreases, the spectral indications and the characteristics of the surface atoms and ions become increasingly sharper. As the disparity of the particle increases, become broader and the absorption bands get frequency shifted.

In the case of nanoparticles the surface envelope whose composition may be different from that of the core could be responsible for the appearance of significant surface tension and corresponding compressive or tensile stresses in the particle. Its effect is significant if there is sharp difference in the elastic constants of one or another region of the particle. The shift in the vibrational lines accompanying a change in pressure is a direct consequence of the an harmonicity of real vibrations.

For the nanocrystalline Mg $(OH)_2$ sample, two additional peaks around 1094 cm^{-1} and 152 cm^{-1} which do not corresponds to any of the first-order Raman lines, are obtained. For nanoparticles the surface-to-volume ration has a large value. Here as the size of the particles decreases, the contribution to the Raman spectral from surface layers increases and new signals may appear in the Raman spectrum. The additional bands in the Raman spectrum of nanostructured $Mg(OH)_2$ may be due to surface vibrational mode. Surface atoms vibrate in an environment different from that of bulk atoms and so the force field to which atoms are subjected at the surface is different form that in the bulk. This could increase the rms amplitude of the oscillation and hence the mechanical anharmonicity. This will affect the Raman scattering spectra from surface layers. Intensity of surface modes increases as the dispersity of the particles increases. Since the surface modes decay very rapidly into the crystal, their intensity should be determined entirely by the surface layer of the particles.

Some of the peaks of the Raman spectrum of the nanocrystalline $Mg(OH)_2$ are wider compared to those of the bulk crystals. As the particles become smaller they become structurally disordered. A particle becomes amorphous in the surface layer while the core retains a crystalline structure. The amorphous structural component of the particles affects the Raman signals. This indicates that the structure of the particles responsible for them is amorphous. Different materials have different critical particle sizes for which the formation of amorphous structure starts. The broadening of bands may also be caused by the decay of phonons. The asymmetry of the lies 712 and 1094 cm^{-1} may be attributed to the dependence of Raman spectrum on the shape of the particles.

From the above discussion it is clear that the nanostructured $Mg(OH)_2$ samples shows optical features which are different from those of bulk $Mg(OH)_2$ crystals. In the Raman scattering spectrum of nanocrystalline $Mg(OH)_2$ two additional peaks which are not reported in the Raman spectrum of bulk $Mg(OH)_2$ are observed. These peaks may be due to surface vibrational modes.

3.2 MgO

(i) X-ray diffraction pattern

The X-ray diffraction pattern of nanoparticles of samples X_1, X_2, M_1, M_2 are shown in fig.5, 6, 7 and 8. The diffraction peaks indicate that all the four samples are crystalline in nature. The d values and intensity of peaks are compared with JCPDS values of $Mg(OH)_2$ crystals and MgO crystals. The JCPDS data of MgO crystal is given in the Table 4.

Table 4: JCPDS data of MgO crystal

d (A)	I	h	k	l
2.43163	4	1	1	1
2.10564	100	2	0	0
1.48905	39	2	2	0
1.26982	5	3	1	1
1.21578	10	2	2	2
1.05281	8	4	0	0
0.196621	2	3	3	1
0.94272	19	4	2	0
0.85967	14	4	2	2
0.181051	4	5	1	1

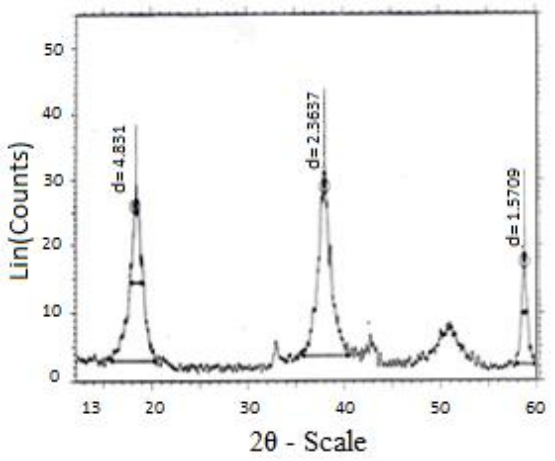

Figure 5: XRD spectrum of sample X_1

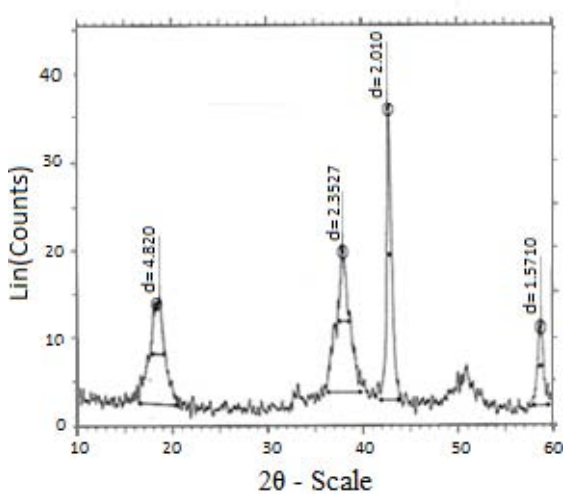

Figure 6: XRD spectrum of sample X_2

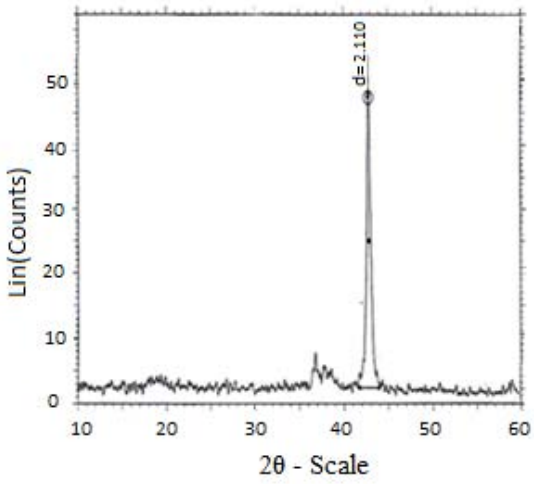

Figure 7: XRD spectrum of sample M_1

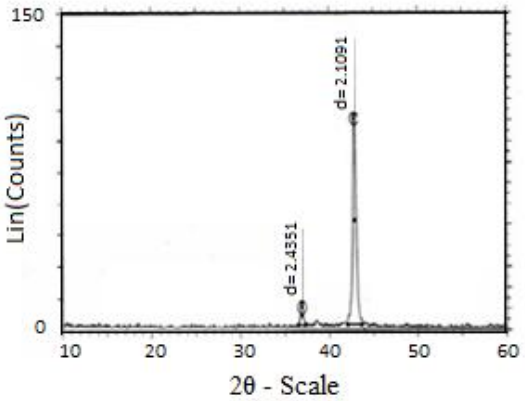

Figure 8: XRD spectrum of sample M_2

The comparison gave the result that X_1 resembles exactly with $Mg(OH)_2$. Even though the sample was annealed for one hour, it had not transformed into MgO. X_2 has the characteristic peaks of both $Mg(OH)_2$ and MgO. The sample started to transform into MgO. M_1 and M_2 are the sample which have almost completely transformed into MgO. Trace of Mg $(OH)_2$ is present in M_1 and M_2 as indicted by the appearance of the strongest XRD peak corresponding to $Mg(OH)_2$ in the XRD patterns of M_1 and M_2 as a very weak peak. Using Scherer's formula the average particles sizes of samples are calculated and they are given in the table 5.

Table 5: Average particle size of MgO nanoparticles

Sample code	Size in nm
M_1	20
M_2	23

Both samples of MgO are nanocrystalline. From the above table, it is evident that as annealing temperature increases, the average grain size of nanocrystalline materials also increases. The width of the X-ray diffraction patterns indicates the same results.

The samples M_1 and M_2 are used for the Raman spectroscopic study.

(ii) Raman Scattering Spectra

FT Raman spectra of nanostructured samples of MgO of particle sizes 20 and 23 nm (samples M_1 and M_2) are shown in figure 3.7 & 3.8.

Since MgO has a sodium chloride structure with inversion symmetry, first-order Raman scattering is forbidden in large bulk crystals. Only second-order Raman spectrum has been observed in bulk crystals, and it can be well understood with the aid of theoretical treatments.

But there are reports of the observation of first order Raman scattering in microcrystals of MgO. First order Raman peaks have been observed in microcrystals of MgO by Ishikawa et al. around 280, 446, and 1088 cm^{-1}, the 446 cm^{-1} peak being the strongest. In the present study, a weak peak has been observed in the spectrum of sample M_1, around 448 cm^{-1}. This can be attributed to first order Raman scattering in comparison with the report of Ishikawa et al. The weak peak observed by Ishikawa et al around 280 cm^{-1} has not be observed, probably due to the very small intensity of this peak in the present study, where as the peak around 1088 cm^{-1} was not observed. No peaks were observed in spectrum of the sample M_2, obtained by heat treatment of $Mg(OH)_2$ sample at a higher temperature of 600 C for 2 hours.

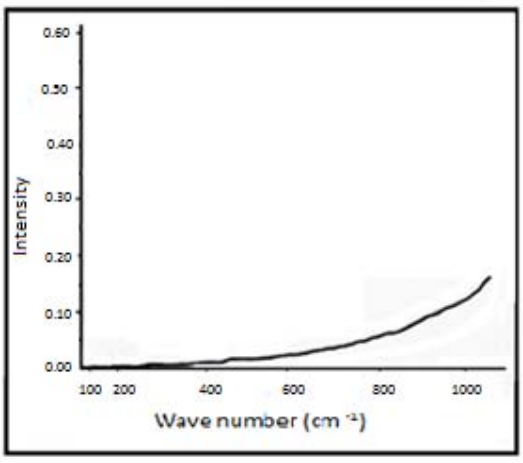

Figure 9: FT Raman spectrum of sample M_1

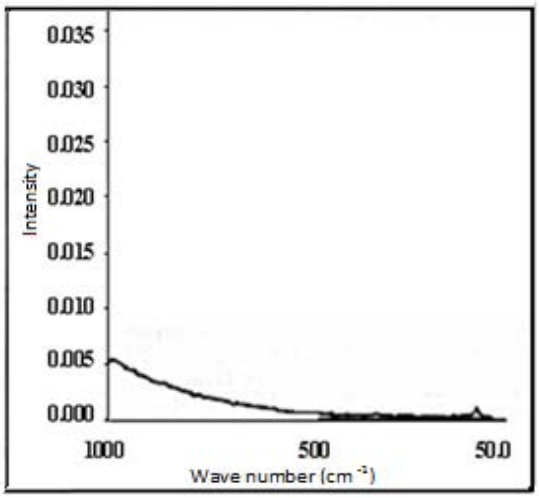

Figure 10: FT Raman spectrum of sample M_2

Brockelman et al reported first order Raman spectrum having peaks at 579, 719 and 1096 cm^{-1} in the case of microcrystals of MgO of particle sizes 10-30 nm. These peak positions obeyed inverted Lyddane-Sachs-Teller relation. The microscopic theory of MgO crystals uses Maxwell's equations with appropriate boundary conditions.

If ε_o and ε_α represent static and high frequency dielectric constants of a specimen and if ω_{TO} and ω_{LO} are the transverse-optical and longitudinal-optical frequencies of the corresponding infinite crystal respectively. Fr ö hlich obtained (Fröhlich mode):

$$\left(\omega^2/\omega^2\right) = \left((\varepsilon_0 + 2)/(\varepsilon_\alpha + 2)\right) \quad \ldots (1)$$

UsingLyddane-Sachs-Teller relation

$$\left[(\omega/\omega) = (\varepsilon_0/\varepsilon_\alpha)^{(1/2)}\right],$$

$$\left(\omega^2/\omega^2\right) = \left[(\varepsilon_0/\varepsilon_\alpha)\left((\varepsilon_0 + 2)/(\varepsilon_\alpha + 2)\right)\right] \quad \ldots (2)$$

Since $\varepsilon_o < \varepsilon_\alpha$ the so-called Fröhlich mode was for an ionic crystals, falls in the transverse-optical-longitudinal-optical gap (TOLOG). These calculations hold good in the case of MgO microcrystals having sizes ranging from 60 to 300 nm in the experiment of Brockelman et al.

Ishikawa et.al have reported the first order Raman scattering in MgO microcrystals. They observed peaks around 280, 446, and 1088 cm^{-1}. These peaks are absent in the Raman spectrum of bulk MgO crystals.

In the present work, for the sample M_1 a peak at 448 cm^{-1} was obtained. This peak is in close agreement with the intense peak obtained by Ishikawa et al. The explanation offered by Ishikawa et al for the observation of first order Raman scattering in microcrystals of MgO, which is forbidden in bulk crystals of MgO, is applicable in the present study also. The other two peaks (280 cm^{-1}, 1088 cm^{-1}) in Ishikawas work could not be observed in the present work. This may be due to the very small intensity of these lines.

In the work of Ishikawa et al the strongest peak around 446 cm^{-1} is attributed to the contribution from a transverse optical (TO) phonon and another weaker peak around 280 cm^{-1} to a transverse acoustic (TA) phonon. The frequency of one-phonon Raman spectrum of microcrystalline MgO was calculated by Chen. The line at 280 cm^{-1} and 446 cm^{-1} coincide with the two prominent peaks in Chen's calculations. 446cm^{-1} line relates to TO phonon at the zone centre and the 280 cm^{-1} line relates a TO phonon at zone boundary. The 280 cm^{-1} peak should be classified as Brillouin scattering since an acoustic phonon is relevant to the scattering process.

The observed one phonon Raman lines are forbidden in the Bulk MgO, although Raman lines due to two TO and two TA phonons are observed in single crystals. The selection rule is relaxed by the reduction of crystal symmetry in particles. In addition, momentum conservation is not satisfied for 280 cm^{-1} like since a TA phonon at the Brillouin zone edge participates the scattering process. Symmetry reduction may occur by the distortion in the surface regions of the nanoparticles. Such a surface effect can be expected in Ishikawa et al's work. The above explanations may be valid in the present case also.

In the case of sample M_2 with average grain size of 23 nm, the first order Raman peaks were not observed. This may be due to the increase in average particle size by annealing. The mode of preparation of sample can also affect the position and intensity of peaks. As the particle size increases, surface affects decreases considerably. Due to this factor, intensity of one-phonon Raman peaks may decrease.

3.4 Conclusion

The nanoparticles $Mg(OH)_2$ was prepared by chemical precipitation method. Nanoparticles of MgO of two different particle size were obtained by thermal treatment of the $Mg(OH)_2$ sample. X-ray diffraction was made use of in determining the structure and grain size of the samples. The FT Raman spectra of nanoparticles of Mg $(OH)_2$ and the two samples of MgO were recorded. The spectra are discussed in comparison with the reported Raman Spectra of corresponding single crystals and/or microcrystals.

References

[1] Hari Singh Nalwa (Ed) Handbook for Nano structured Materials and nanotechnology volume 1-V academic press USA (2000).
[2] R. Birringer, H. Gleiter, H.P. Klein and P. Marquardt, Phys. Lett. 102 (1984) 365.
[3] C. Suryanarayana, Bull. Mater. Su 17 (1994) 307.
[4] W.M. Tolles and B.P. Rath, Curr. Sc. 85 (12) 2013, 1746.
[5] S. Komarneni, Nanophase Materials In M.C. Graw – Hills year book of science and technology M.C. Graw Hill New York (1995) 285.
[6] Sridhar Komerneni, Curr. Sci. 85(12) (2003) 1750.
[7] A D yoffe, Adr. Phys. 42 (1993) 173. Various Characterization techniques.
[8] R.W. Seigel, nanostruct. Mater. 4 (1991) 121.
[9] J Norton, K R Malik, J A Darr and Rehman, Adv. Appl. Ceram 105 (2006) 113.
[10] Nanotechnology (volume 1 to 5) – Naveen kumar Navani, Shishir Sinha.
[11] D Castner and B Ratner, Surf. Sci. 500 (2002) 28.

[12] Nanotechnology 101 – John Mongolloid.
[13] Rodrigues J A & Fernandez –Garcia M, Synthesis, Properties and Applications of Oxide Nanomaterials, (John Wiley & Sons, New Jersy) 2007.
[14] Drissen M D, Miller T M & Grassian V H, J MolCatal A: Chem, 131 (1998) 149.
[15] Villaseoor J, Reyes P &Pecchi G J, Chem Technol Biotechnol, 72 (1998) 105.
[16] Yeber M C, Rodriguez J, freer J, D Durian N &Mansilla H D, Chemosphere, 41 (2000) 1193.
[17] Diao Y, Walawender W P, Sorenson C M, Klabunde K J & Ricker T, Chem Matter, 14 (2002) 362.
[18] Wagner G W, Koper O, Lucas E, Decker S &Klabunde K J, J PhysChem B, 104 (2000) 5118.
[19] Rajagopalan S, Koper O, Decker S & Kiabunde K J, ChemEur J, 8 (2002) 2602.
[20] Interrante L & Hampden-Smith M, Chemistry of Advanced Materials, (Wiley-VCH, New york) 1998, pp. 271-327.
[21] Jeevanandam P &Klabunde K J, Langmuir, 18 (2002) 5309.
[22] Lide D R, CRC Handbook of Chemistry and Physics. A Ready-Reference book of Chemical and Physical Data, 77thEdn, (CRC, Press, Boca Raton – New York – London ToKyo) 2004.
[23] Choi H S & Hwang S T, J Mat Res, 15 (2000) 842.
[24] Lopez T, Gomez R, Navarrete, J & Lopez- Salinas E, J Sol-Gel Sci Tech, 13 (1998) 1043.
[25] Stark, J V & Klabunde K J, Chem Mater 8 (1991) 1913.
[26] Znaidi L, Chhor K & Pommier C, Mat Res Bull, 31 (1996) 1527.
[27] Hattori T, Matsumoto H &Mohri J, J Mater Sci let, 2 (1983) 503.
[28] Cullity B D, Elements of X-Ray Diffraction ^{2nd}Edn, (Addison-Wesley Publishing Company Inc., California) 1978, p. 102.
[29] Hubert-Pfalzgraf L G, New J Chem, 11 (1987) 663.
[30] Schmidt H, J Non- Cryst Solids, 100 (1988) 51.